The primary photolysis of aqueous hydrogen carbonate and carbonate anions.

Jan Thøgersen, Tobias Weidner and Frank Jensen.

Supplementary information.

Singular value decomposition of the absorption associated with CO_3^{2-} and $CO_3^{\bullet-}$

Since the absorption dynamics of CO_3^{2-} and $CO_3^{\bullet-}$ are distinctly different, Singular Value Decomposition (SVD) of the data can possibly extract the absorption spectra and dynamics of the entangled spectral system of the two species. The SVD analysis using three spectral components gives an accurate description of the experimental transient absorption dynamics, illustrated by the contour plot of the SVD analysis in Fig. SI 1b being nearly indistinguishable from the experimental transient absorption data in Fig. SI 1a. The SVD analysis finds a spectral component shown in Fig. SI 1c, which peaks at $\nu = 1400$ cm^{-1} and has spectral properties similar to those of ground state $CO_3^{2-}(D_2O)$ shown in Fig. 2b, and we assign this SVD spectral component to ground state CO_3^{2-}. The time dependent absorption associated with this spectral component is shown in Fig. SI 1d. The SVD absorption dynamics drops to a minimum in t = 1.4 ps after the excitation pulse and partially recovers to 78 % of its maximum (negative) absorption change on a $\tau = 5.2 \pm 0.3$ ps time scale. The SVD analysis finds a second spectral component shown in Fig. SI 1e with a maximum at $\nu = 1360$ cm^{-1} and a smaller (negative) minimum around $\nu = 1410$ cm^{-1}. The second SVD component is shifted to the low frequency side (red-shifted) of ground state $CO_3^{2-}(D_2O)$ and its absorption dynamics in Fig. SI 1f show a monotonous decay with a decay constant of $\tau = 4.6 \pm 0.5$ ps, comparable to the $\tau = 5.2 \pm 0.3$ ps recovery time of the ground state absorption. The spectral behavior of this second SVD component is thus in line with that expected for vibrationally relaxing CO_3^{2-} predicted by the analysis above. Due to the anharmonicity of the ground state potential, vibrational relaxation towards equilibrium is characterized by a continuously blue-shifting absorption feature on the low-frequency side of the equilibrated ground state absorption. By construction, the SVD analysis identifies the spectral components characterized by having identical temporal behavior. The temporal dynamics of time-dependent spectral shifts, as those of vibrational relaxing molecules, are not identical and may therefore introduce ambiguity in the analysis and affect other spectral components. The third SVD component shown in Fig. SI 1g has a maximum at $\nu = 1440$ cm^{-1} and resemble the spectrum assigned to $CO_3^{\bullet-}$ in Fig. 8a. The SVD analysis thus finds the same spectral component as the approach used in the previous section, but the time dependent absorption dynamics of the third SVD component in Fig. SI 1h is distinctly different from the constant absorption assigned to $CO_3^{\bullet-}$ in Fig. 8b. The reason for this difference is unclear, but the third SVD component may be perturbed by inaccuracies introduced by the two larger components, and the time dependence of the third component could be an artifact introduced by the spectral shifts of the vibrationally relaxing CO_3^{2-} di-anions. Performing the SVD analysis with (only) two components identifies only the ground state and relaxing CO_3^{2-} di-anions, while adding a fourth component results in an undulating behavior covering the entire spectrum with an amplitude one order of magnitude less than those with two or three components. The data thus warrants a three component SVD analysis, with the third component assigned to $CO_3^{\bullet-}$.
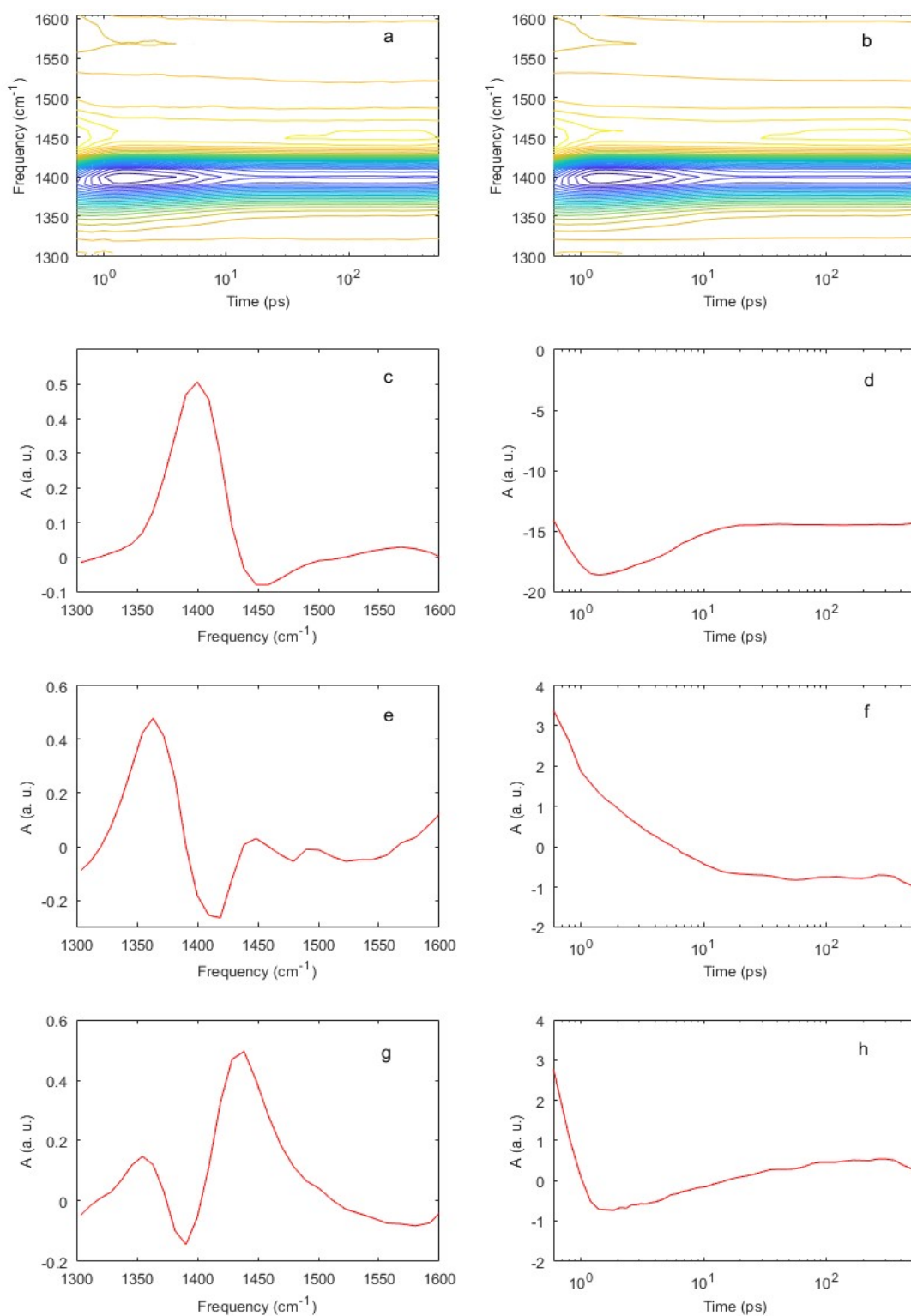
Fig. SI 1. SVD analysis of the experimental data associated with the symmetric and asymmetric stretch of $CO_3^{2-}(D_2O)$ and $CO_3^{\bullet-}(D_2O)$. a) Experimental transient absorption. b) Transient absorption data calculated by three-component SVD analysis. c) SVD spectrum assigned to ground state CO_3^{2-}, d) SVD absorption dynamics assigned to ground state CO_3^{2-}. e) SVD spectrum assigned to vibrationally relaxing CO_3^{2-}. f) SVD absorption dynamics assigned to vibrationally relaxing CO_3^{2-}. g) SVD spectrum assigned to $CO_3^{\bullet-}$. h) SVD absorption dynamics assigned to $CO_3^{\bullet-}$
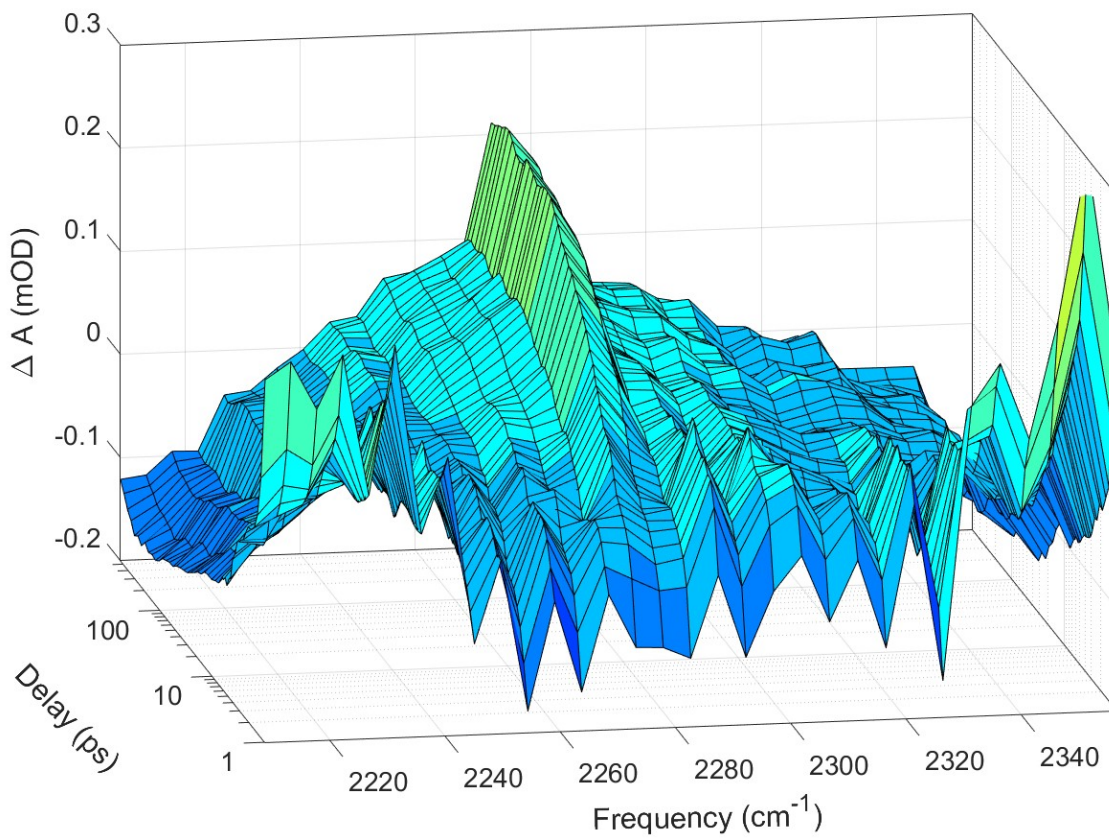
Fig. SI 2. Formation of $^{13}CO_2$(aq) after the photo-dissociation of $^{13}CO_3^{2-}$(aq).

Excitation of ground state HCO$_3^-$(aq)

Fig. SI 3 shows the transient infrared absorption dynamics from ν = 1260 cm^{-1} to ν = 1840 cm^{-1} and from ν = 2250 cm^{-1} to ν = 2430 cm^{-1} following the photoexcitation of the aqueous hydrogen carbonate solution at λ = 200 nm. Transient absorption data recorded in the interval ν = 1000 cm^{-1} - 1300 cm^{-1} are not shown, since they only contain photo-induced absorption changes of the solvent similar to those in Fig. 7 for carbonate. Fig. SI 3b shows the induced transient absorption from ν = 1440 cm^{-1} to ν = 1840 cm^{-1} together with the IR spectrum of equilibrated ground state HCO$_3^-$(aq). The transient absorption data is dominated by the negative absorption change at ν = 1625 cm^{-1} associated with the HCO$_3^-$(aq) asymmetric stretch transition. The absorption dynamics exemplified by the transient at ν = 1612 cm^{-1} is shown in Fig. SI 3a, with the absorption dropping to ΔA(t = 1 ps, ν = 1612 cm^{-1}) = -1.1 mOD within t = 1 ps after the excitation, indicating the prompt photo-excitation of ground state hydrogen carbonate. However, contrary to what is expected from photo-excitation dynamics, the negative transient absorption keeps decreasing with time after the photo-excitation has finished indicating that secondary reactions continuously remove ground state HCO$_3^-$(aq) molecules after the initial photoexcitation. The decreasing transient absorption is well approximated by a double exponential function with time constants of τ_1 = 7.8 $\pm$ 0.5 ps and τ_2 = 366 $\pm$ 126 ps.
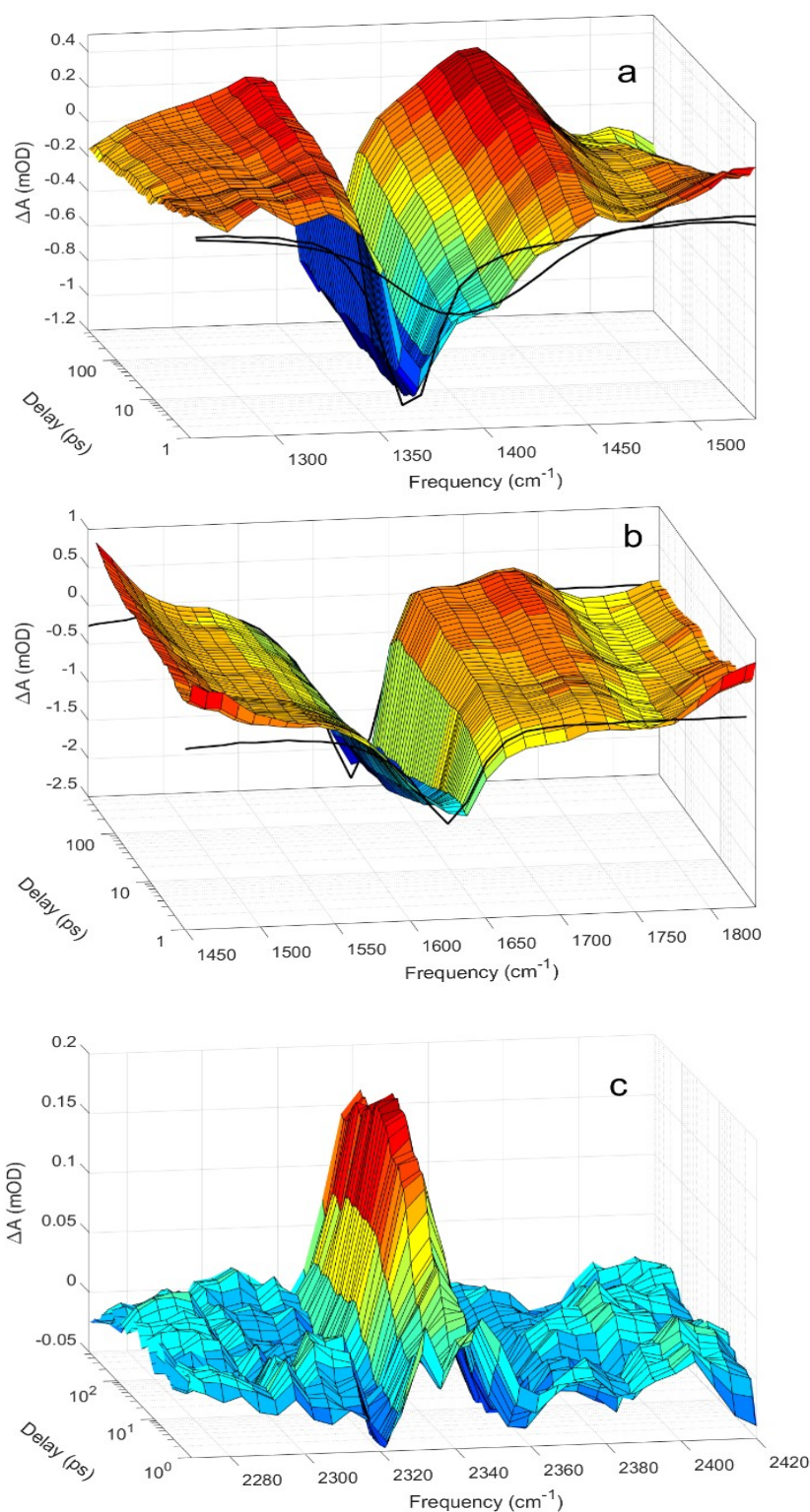
Fig SI 3. Selected transient absorption spectra from the aqueous hydrogen carbonate sample recorded as a function of time after the $\lambda = 200$ nm excitation pulse. The IR spectra of HCO_3^-(aq) and CO_3^{2-}(aq) are shown for comparison. a) The negative absorptions with minimum at $\nu = 1360$ cm^{-1} and $\nu = 1400$ cm^{-1} reflect the excitation of ground state HCO_3^-(aq) and CO_3^{2-}(aq), respectively. The wide positive absorption with maximum at $\nu = 1446$ cm^{-1} is assigned to $CO_3^{\bullet-}$(aq) and H_2CO_3(aq). b) The transient negative absorption associated with asymmetric stretch transition at $\nu = 1625$ cm^{-1} indicates the excitation of ground state HCO_3^-. The steep absorption flank around $\nu = 1630$-1650 cm^{-1} reveals a positive absorption at $\nu = 1627$ cm^{-1} assigned to the asymmetric stretch of $CO_2^{\bullet-}$(aq). The positive induced absorption centered at $\nu = 1720$ cm^{-1} indicates the formation of H_2CO_3(aq). c) The positive absorption at $\nu = 2341$ cm^{-1} is assigned to the formation CO_2(aq). The transient absorption of the three

The symmetric CO_2 stretch of $HCO_3^-(aq)$ at $\nu = 1360$ cm^{-1} displays the same prompt excitation dynamics of $HCO_3^-(aq)$ as the asymmetric stretch at $\nu = 1625$ cm^{-1}. Fig. SI 3a shows the transient absorption data from $\nu = 1260$ cm^{-1} to $\nu = 1554$ cm^{-1} and the corresponding IR spectra of equilibrated $HCO_3^-(aq)$ and $CO_3^{2-}(aq)$. At t = 1 ps the transient absorption data is dominated by the negative absorption change at $\nu = 1360$ cm^{-1}. The transient data at t = 1 ps shows a second negative absorption change with minimum at $\nu = 1400$ cm^{-1} reflecting the excitation of the inevitable carbonate di-anions in the sample. At t = 1 ps there is a weak positive absorption at $\nu = 1446$ cm^{-1} signifying the prompt formation of photo-products. This absorption increases monotonously throughout the duration of the measurement and judging by a similar increase in the absorption around $\nu = 1340$ cm^{-1}, it stretches across the negative absorption change pertaining to ground state hydrogen carbonate. Accordingly, the nearly constant negative absorption measured at $\nu = 1360$ cm^{-1} is in fact the sum of a positive, increasing absorption from a yet undetermined species and a negative, decreasing absorption related to ground state hydrogen carbonate. The decreasing negative absorption change associated with the symmetric CO_2 stretch of ground state hydrogen carbonate at $\nu = 1360$ cm^{-1} is in line with the decreasing absorption associated with asymmetric CO_2 stretch of ground state hydrogen carbonate observed at $\nu = 1625$ cm^{-1}.

The formation of $CO_2^{\bullet-}(aq)$

The high frequency slope of the negative absorption change at $\nu = 1625$ cm^{-1} is significantly steeper than the corresponding slope of the steady state infrared absorption. The difference reveals a positive absorption contribution around $\nu = 1630\text{-}50$ cm^{-1}. This absorption is at least in part due to the formation of $CO_2^{\bullet-}(aq)$ from photo-dissociation of $CO_3^{2-}(aq)$ as described in previous sections. The $CO_2^{\bullet-}(aq)$ anion may also result from the photo-dissociation of $HCO_3^-(aq)$:

$$h\nu + HCO_3^- \rightarrow CO_2^{\bullet-} + OH^\bullet$$

(14)

However, the absorption dynamics on the $\nu = 1630\text{-}50$ cm^{-1} slope is too weak to assess if it contains $CO_2^{\bullet-}(aq)$ contributions other than those produced by photo-dissociation of $CO_3^{2-}(aq)$ shown in Fig. 7e. Whether photo-dissociation of $HCO_3^-(aq)$ yields $CO_2^{\bullet-}(aq)$ therefore remains an open question.

The formation of $H_2CO_3(aq)$

The transient absorption data in Fig. SI 3b furthermore shows a positive induced absorption centered at $\nu = 1720$ cm^{-1} indicating the
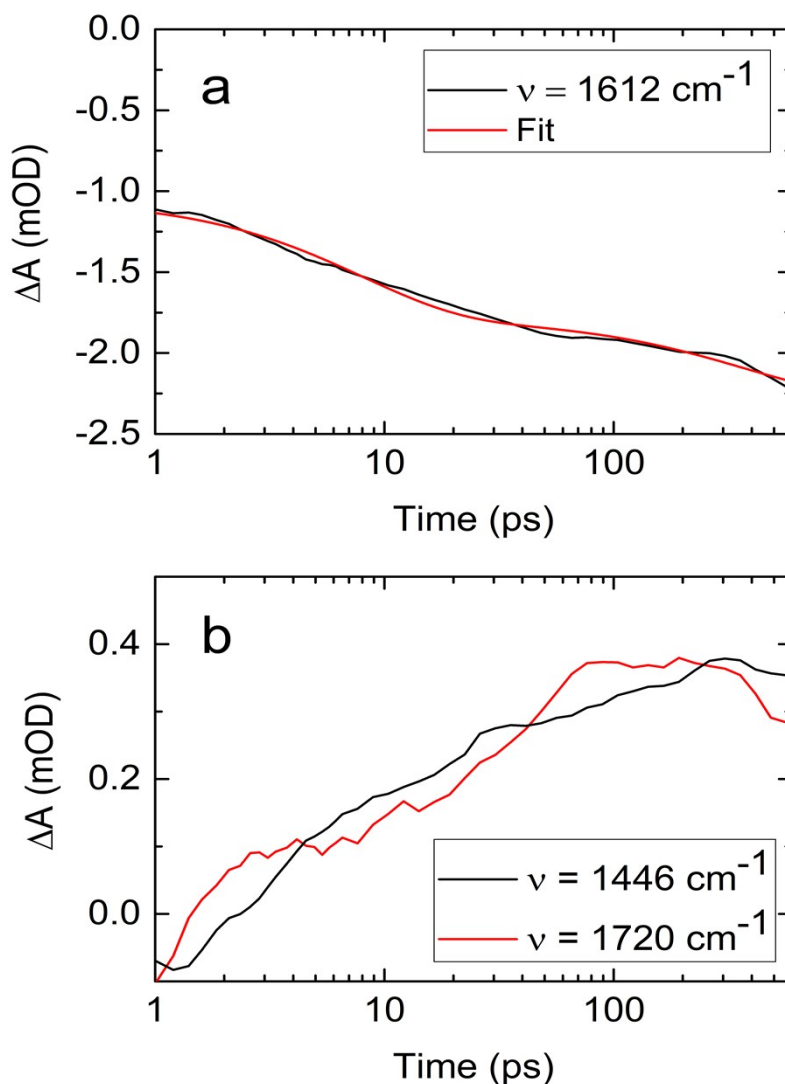
Fig. SI 4. Time dependence of the transient absorption associated with a) the ground state absorption from hydrogen carbonate b) carbonate anion radical and carbonic acid.

formation of a true carbonyl like carbonic acid. At first the absorption is only slightly above the background level, but it increases with time during most of the measurement. Carbonic acid has according to our calculations two strong transitions within the investigated spectral range, one at $\nu = 1747$ cm^{-1} with an intensity of I = 338 km/mol and one at $\nu = 1424$ cm^{-1} with an intensity of I = 187 km/mol. Within the accuracy of the calculations, these frequencies agree with the measured value of $\nu = 1720$ cm^{-1} and thereby support the assignment to carbonic acid and furthermore predict a carbonic acid transition around $\nu = 1424$ cm^{-1}. As mentioned above, the transient absorption depicted in Fig. SI 3a includes a wide positive absorption peak with maximum at $\nu = 1446$ cm^{-1}. The absorption increases from a finite positive value throughout the duration of the measurement and likely spans the frequency interval $\nu = 1330$ -1460 cm^{-1}. After t $\approx$ 10 ps the positive absorption dominates the negative absorption associated with the ground state carbonate di-anions, which in the meantime has dropped by about 20 % for reasons discussed in the *Excitation of ground state CO_3^{2-} and the formation of $CO_3^{\bullet-}$* section. The prompt absorption at $\nu = 1446$ cm^{-1} is partly due to $CO_3^{\bullet-}$ formed by the electron photo-detachment of CO_3^{2-} described above, but the prompt electron detachment does not explain why the absorption keeps increasing after the initial excitation. The increasing part of the absorption likely has two contributions: As mentioned in the *Theoretical considerations* section, our calculations indicate that the pK_a of HCO_3^-(aq) drops by ~19 units upon excitation and deprotonation of excited HCO_3^-(aq) to $CO_3^{\bullet-}$ is therefore expected to succeed the photo-excitation for as long as the excited state is populated. In addition, the wide absorption with maximum at $\nu = 1446$ cm^{-1} contains a contribution from carbonic acid. Fig. SI 4b compares the

dynamics of the transient absorption at ν = 1446 cm^{-1} and ν = 1720 cm^{-1}. Within the experimental uncertainty the dynamics of two traces are comparable and suggests that the major part of the transient absorption at ν = 1446 cm^{-1} is due to the formation of carbonic acid.

The absorption dynamics associated with ground state HCO$_3^-$(aq) points to the formation of carbonic acid. Fig. SI 4a shows the absorption dynamics of ground state HCO$_3^-$(aq) exemplified by the absorption at ν = 1612 cm^{-1}. We note that the slow formation of carbonic acid occurs on a time scale resembling that of the slow removal of ground state hydrogen carbonate, suggesting that the continuous removal of ground state hydrogen carbonate is related to the formation of carbonic acid. The formation mechanism of carbonic acid becomes clear when analyzing the intensity dependence of the absorption transients associated with the H$_2$CO$_3$(aq) formation.

Fig. SI 5a shows the intensity dependence of the transient absorption associated with the asymmetric stretch transition of ground state HCO$_3^-$(aq) recorded t = 2 ps, t = 50 ps and t = 514 ps after the excitation pulse. All three curves show a non-linear intensity dependence indicating that the removal of ground state HCO$_3^-$(aq) has a quadratic intensity component. The quadratic component

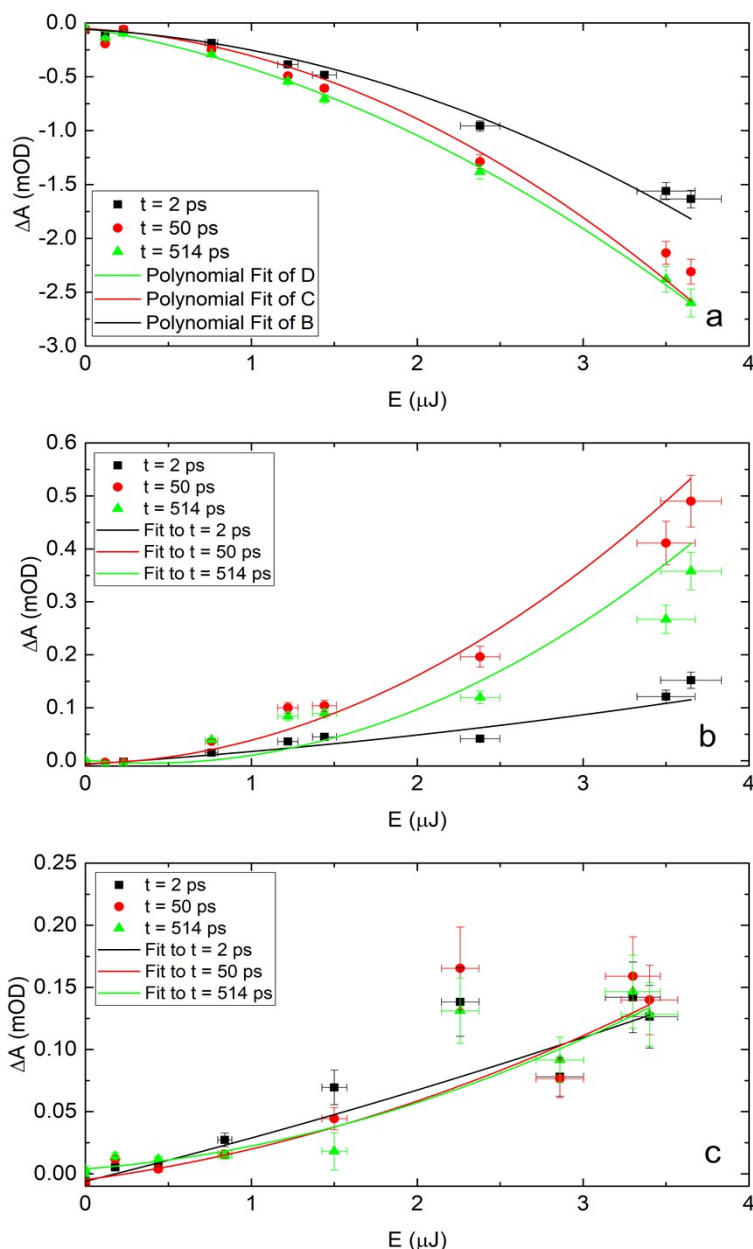
Fig. SI 5. Intensity dependence of the transient absorption associated with the formation of carbonic acid recorded t = 2 ps, t = 50 ps and t = 514 ps after the excitation pulse. a) The asymmetric stretch transition of ground state HCO$_3^-$(aq) at ν = 1612 cm^{-1}. b) The carbonic acid formation represented by the transient absorption at ν = 1719 cm^{-1}. c) The carbonic acid formation represented by the transient absorption at ν = 1446 cm^{-1}.

is least significant after t = 2 ps, where the excitation of HCO_3^-(aq) predominantly results from prompt one-photon excitation. At later times the quadratic component increases indicating that secondary reactions with reactants produced by two-photon excitation become increasingly more important. As mentioned in the *Electron photo-detachment of the HCO_3^- (aq) solution* section above, such reactants could be hydronium cations produced by two-photon ionization of water. This scenario is confirmed by the measurement of the intensity dependence of the carbonic acid formation represented by the transient absorption at ν = 1719 cm^{-1} in Fig. SI 5b. At t = 2 ps after the photoexcitation, the intensity dependence of the weak residual solvent absorption at ν = 1719 cm^{-1} is essentially linear, but changes dramatically with time. The recorded absorption after t = 50 ps and t = 514 ps both show a strong quadratic intensity dependence in line with the notion that H_2CO_3(aq) is formed by protonation of HCO_3^-(aq) by H_3O^+ cations produced by two-photon ionization of water. The same intensity dependence after t = 2 ps, t = 50 ps and t = 514 ps is also found at the second transition frequency of carbonic acid at ν = 1446 cm^{-1}, even though this transition is associated with a number of species and the signal to noise ratio is poorer than that at ν = 1719 cm^{-1}. We therefore conclude that hydronium cations produced in the process of two-photon ionization of water solvent molecules react diffusively with ground state hydrogen carbonate anions to produce carbonic acid:

$$2h\nu + H_2O \overset{H_2O}{\rightarrow} H_3O^+ + OH^\bullet + e_{aq}^-$$

(15)

$$H_3O^+ + HCO_3^- \rightarrow H_2CO_3 + H_2O$$

(16)
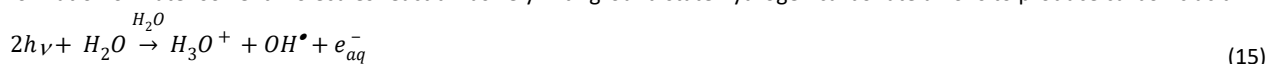
A similar protonation scenario has been reported in the case of protonation of aqueous alanine.[SI 1]

Formation of CO_2(aq)

Fig. SI 3c shows the formation of aqueous carbon dioxide characterized by the absorption at ν = 2343 cm^{-1} when the hydrogen carbonate solution is photo-excited at λ = 200 nm. Fig. SI 6 compares the carbon dioxide absorption dynamics in the hydrogen carbonate solution to that observed in the carbonate solution. The two absorption traces are similar within the experimental uncertainty. Accordingly, the observed CO_2(aq) most likely stems from the photolysis of the carbonate component of the hydrogen carbonate solution. Whether hydrogen carbonate dissociates to CO_2 and OH^- as predicted by our theoretical consideration remains an open question.
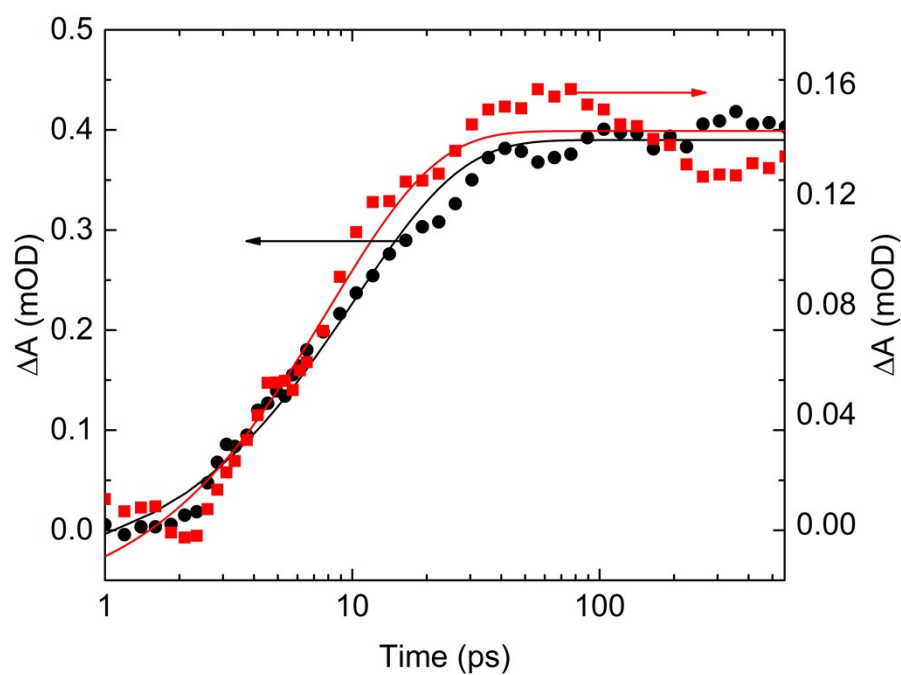
Fig. SI 6. Comparison of the CO_2(aq) absorption dynamics in the carbonate solution (black) and hydrogen carbonate solution (red). The data are fitted with single exponential functions with time constants of τ = 10.2 ± 0.5 ps and τ = 8.1 ± 0.6 ps, respectively.

References:

1 J. Thøgersen, A. Coletta, S. R. Keiding, F. Jensen, N. Jones, S. V. Hoffmann and S. J. Knak Jensen. *Phys.Chem.Chem.Phys.*, 2017, **19**, 1560.